



Forming of rail car axles in a CNC skew rolling mill

Zbigniew Pater¹ · Janusz Tomczak¹ · Konrad Lis¹ · Tomasz Bulzak¹ · Xuedao Shu²

Received: 25 February 2020 / Revised: 26 April 2020 / Accepted: 28 May 2020 / Published online: 8 June 2020
© The Author(s) 2020

Abstract

This study relates to an innovative method for forming rail car axles by skew rolling in a CNC 3-roll mill. The rolling mill was constructed at the Lublin University of Technology. The use of this machine makes it possible to produce elongated axisymmetric parts that are up to 55 mm in diameter and up to 1000 mm in length. Experimental rolling tests are performed (in 1:5 scale) using this machine. Two types of axles are analysed: one manufactured in accordance with North American standards (AAR Class E) and one manufactured in compliance with European standards (BA302). Diameters of produced axles have a dimensional accuracy of ± 0.4 mm. Produced axles are free from internal cracks, and their surface defects (shallow helical grooves) can easily be removed by machining. The major shortcoming of the proposed method is the presence of chucking allowance. To eliminate this allowance, it is proposed that the forming process should be performed in two operations: rolling extrusion and skew rolling. Results of a numerical analysis were performed using the Simufact.Forming program confirms that rail car axles can be formed by the proposed method.

Keywords Skew rolling · Rail car axle · CNC rolling mill · Experiment · FEM

1 Introduction

Rail car axles are large-size parts manufactured in batches of up to thousands units [1, 2]. These parts are currently produced by open die forging and rotary swaging processes. The open die forging of rail car axles is performed in hydraulic forging presses having a load range between 8 and 15 MN that are coupled with two forging manipulators. In open die forging, car axles are formed from forging ingots with circular or square cross sections, and the manufacturing of a single axle takes several minutes. The duration of the rotary swaging process is shorter (approx. 4 min) due to the use of swaging machines, which also helps reduce machining allowance. The rotary swaging of car axles is performed using rotary swaging machines with 4 dies, each having a load of 6.5 MN [3].

To make the manufacturing of car axles more efficient and less energy-consuming, extensive research is

conducted on the production of these parts by rolling processes. The research focuses on cross-wedge rolling (CWR), a method which is effectively used for producing stepped axles and shafts in the automotive industry [4–6]. Nevertheless, well-known rolling techniques cannot be directly applied to producing rail car axles, as this would require the use of large rolling mills equipped with tools of up to 3 m in diameter [2]. Studies are also conducted on the use of parallel (multi-wedge) cross-rolling for producing car axles. In this method the workpiece is simultaneously deformed by 2 or 3 sets of wedges, which means that the nominal diameter of the tools could be reduced to 1600 mm [1, 7]. Results of the rolling tests performed in 1:5 scale by Peng et al. [7] and Zheng et al. [8] demonstrated that the production of rail car axles by the multi-wedge cross-rolling method is difficult due to significant inaccuracies in product shape and the problem with removing the ovalisation of the cross section of the product (in the case of hollow axles). According to Pater and Tomczak [9], an alternative to multi-wedge cross-rolling is a CWR process that is performed in two operations. The first operation involves forming a step in the centre of the workpiece, while the other involves forming steps on the shaft ends using a different set of tools. As a result, the nominal diameter of the tools can be reduced to 1200 mm,

✉ Zbigniew Pater
z.pater@pollub.pl

¹ Lublin University of Technology, 36 Nadbystrzycka Str,
20-618 Lublin, Poland

² Faculty of Mechanical Engineering and Mechanics, Ningbo
University, Ningbo 315211, People's Republic of China

which has been confirmed numerically. A disadvantage of the above CWR process is a high cost of the tool set (rolls and guides), not to mention the fact that the tool set can be used to produce only one type of axles.

Another method for producing rail car axles is skew rolling with the use of three tapered rolls. Apart from rotating, these tools can also move perpendicularly (radially) relative to the axis of the workpiece. By coupling the motion of the rolls with that of the chuck (which moves in the axial direction) it becomes possible to produce elongated axisymmetric parts of any shape. Preliminary numerical analyses performed by Xu and Shu [2] and Pater et al. [10] have shown that this method can be effectively used to produce axles, both solid and hollow. As it was demonstrated by Pater [11], the skew rolling process requires relatively low loads and torques. An enormous advantage of skew rolling is the fact that the same set of tools (tapered rolls) can be used to produce parts of different shapes [12, 13].

Results of the aforementioned numerical analyses investigating the manufacturing of rail car axles by skew rolling must be validated by experimental tests. Such experiments were performed (in 1:5 scale) for two different types of axles: one produced in compliance with European standards, and the other according to North American standards, as shown in Fig. 1. The scale applied in the experimental tests (1:5) resulted from the performance capability of the CNC skew rolling mill that was specially designed and constructed for this purpose at the Lublin University of Technology. Results of these experimental tests are presented in this paper.

2 Design of the skew rolling process

A schematic design of the skew rolling process performed in a CNC rolling mill is shown in Fig. 2. In this process, a cylindrical rod with a diameter d_0 and a length l_0 is simultaneously deformed by three identical rolls and one chuck. The rolls with a diameter D are positioned every 120° on the circumference of the workpiece. They are positioned askew at the angle θ to the axis of the workpiece. During the forming process, the rolls are rotated in the same direction with the same rotational speed n_R . Due to the skew position of the rolls, the workpiece is rotated in an opposite direction to that of the rolls, and, simultaneously, it is pulled by the rolls into the workspace of the machine. The size of the workspace depends on the forming angle of the rolls, α , and the width of a cylindrical (sizing) part of the rolls, b . The rolls can also move in the radial direction and thus reduce the diameter of the axle step being formed. By coupling the axial motion of the chuck (which moves with a velocity v_C) with the motion of the rolls (which move with a velocity v_R towards the axis of the workpiece) it becomes possible to form long axisymmetric parts such as stepped axles or shafts.

3 Laboratory CNC skew rolling mill

Research conducted at the Lublin University of Technology primarily focuses on rotary forming of axisymmetric parts. The CNC skew rolling mill was designed and constructed as part of this research. The machine design makes it possible to produce elongated axisymmetric parts because the

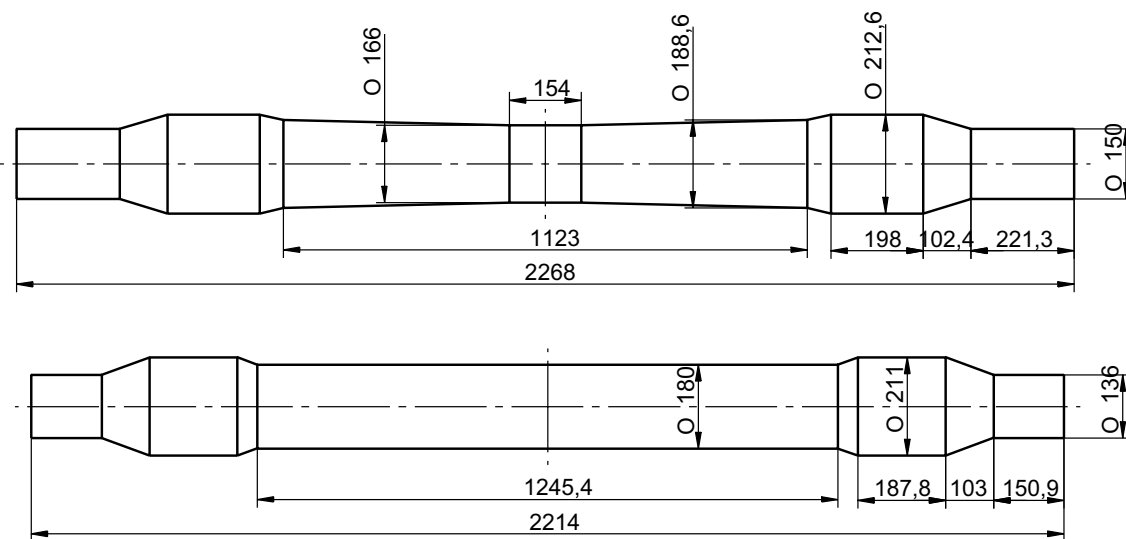


Fig. 1 Analysed rail car axles: (top) axle-type AAR Class E (standard M101); (bottom) axle-type BA302 (Standard EN 13261); the shape of the axles is modified to produce them by skew rolling

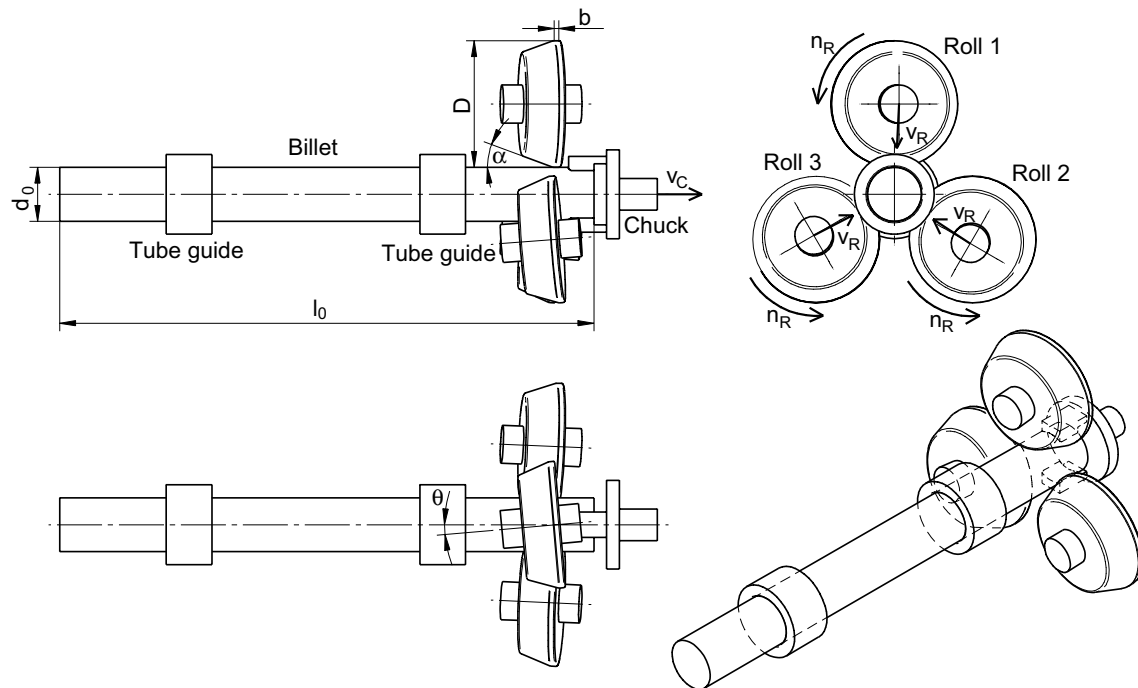


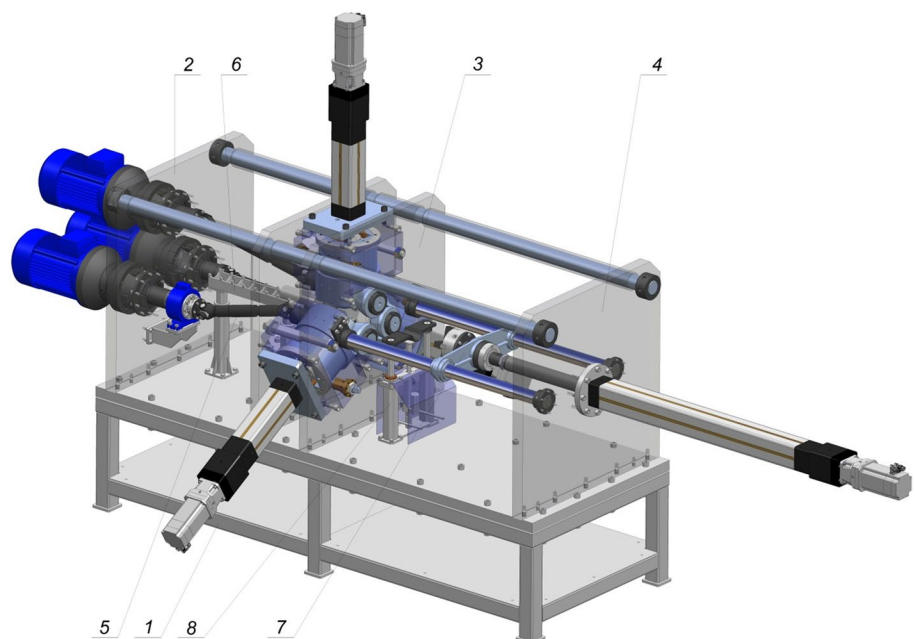
Fig. 2 Schematic design of the skew rolling process for producing rail car axles in the CNC rolling mill (start of the process) and the key parameters of this process

tools can rotate in the same direction and move towards the axis of the workpiece at the same time. As a result, the workpiece motion along the rolling axis can be controlled. The CNC skew rolling mill has a segment structure and consists of nine systems: a frame—1, a drive system—2, a mill stand—3, an axial displacement system—4, a powertrain—5, a workpiece-supporting system—6, a four-jaw

chuck system—7, a product-supporting system—8, and a power and control system. A 3D model of this rolling mill is shown in Fig. 3.

The workpiece (cylindrical rod) is mounted in a head of the workpiece-supporting system. Next, one of its ends is fixed in the four-jaw chuck. The workpiece is moved together with the chuck to the initial position by an electric screw

Fig. 3 3D model of the CNC skew rolling mill (see description in the text)



actuator of the axial displacement system. After that, three tool shafts with the rolls mounted on their necks are set in rotation. Next, three slides are set in translation motion in the axial direction with the use of electric screw actuators. After starting the translational motion of the axial displacement actuator, the chuck and the workpiece begin to move in the axial direction. In addition, the workpiece is rotated by the rotating rolls. The radially rotating tools reduce the cross section of the workpiece. Also, the workpiece is moved axially between the rotating rolls by the chuck system, which leads to the formation of successive steps on the workpiece. The radial motion of the tools is coupled with the translational motion of the chuck such that a trajectory of the tool motion and the chuck axial displacement corresponds to the envelope of the workpiece profile. Towards the end of the rolling process, the product-supporting head, which prevents products from bending, is set in translational motion towards the rolling axis. The torque is measured with a torque sensor located in front of one of the articulated shafts. The load on the roll is measured with the use of a load sensor located in one of the slides. Technical specifications of the CNC skew rolling mill shown in Fig. 4 are given in Table 1.

4 Experimental tests of the skew rolling process for rail car axles

Experimental tests of the skew rolling process for the two analysed types of rail car axles were conducted at the Lublin University of Technology, as shown in Fig. 1. The experiments were performed in 1:5 scale. It should be mentioned that real axles have one more short step that is located between the end step with the smallest diameter and the step with the biggest diameter, which is where the tapered element is made on the tool due to technological reasons.

Table 1 Technical specifications of the CNC skew rolling mill constructed at the Lublin University of Technology

CNC rolling mill specifications		
Motor power	kW	3 × 7.5
Rotational speed of rolls	rev/min	60
Torque on rolls	Nm	1200
Maximum input diameter	mm	55
Minimum output diameter	mm	25
Maximum input length	mm	600
Maximum output length	mm	1000
Maximum load of rolls	kN	50
Maximum load of axial actuator	kN	50
Tool angle control range	°	± 10
Overall dimensions D × S × W	m	5 × 2.5 × 2.5
Machine weight	kg	5000

The tapered element dimensions were selected such to make it possible to form the aforementioned step by machining.

The rolling process was performed with the use of the rolls described by a diameter $D = 150$ mm, a forming angle $\alpha = 20^\circ$, and a sizing element width $b = 12$ mm. The working edges of the rolls were rounded with a radius $R = 5$ mm. The rolls were positioned askew to the axis of the workpiece at an angle $\theta = 5^\circ$. They were rotated with a constant speed of $n_R = 60$ rpm. The tool velocity v_R in the radial direction and the chuck velocity v_C in the axial direction depended on the axle type and dimensions. Two types of the chuck velocity v_C were applied: reduced (approx. 5 mm/s) and normal (ranging 18 ÷ 28 mm/s). The reduced velocity was applied when the tool spacing was changed to change the diameter of the axle being formed. The normal velocity was applied for forming cylindrical parts, while in the case of axles produced in compliance with the North American standard—it was also used for forming central tapered elements

Fig. 4 CNC skew rolling mill constructed at the Lublin University of Technology



of long length and small taper. The radial tool velocity v_R was selected considering the diameter variation, the length of the tapered element, and the applied chuck velocity. In the cases under analysis, this velocity ranged $v_R = 0 \div 7.1$ mm/s.

The tests were performed on cylindrical rods of 43 mm in diameter and two lengths: 405 and 410 mm, for the axles produced in accordance with the North American standard (AAR Class E) and the European standard (BA302), respectively. The rods were made of 42CrMo4 steel.

Prior to rolling, the rods were preheated to 1180 °C in an electric chamber furnace. Next, they were fixed in the four-jaw chuck of the machine. A chucking allowance (a volume of material fixed in the chuck) will be cut off from the product. The workpiece is put inside the workspace of the machine, and the tools and the chuck motion are started. The forming of the required profile of the axle is controlled by the machine programme. After rolling, the product is removed from the chuck and air-cooled. One of the experimental tests performed in the CNC skew rolling mill at the Lublin University of Technology is shown in Fig. 5.

Variations in the temperature during rolling were measured with an infrared camera. An analysis of the data given in Fig. 6 demonstrates that in spite of the long duration of the forming process (almost 40 s), the workpiece does not undergo much cooling and its temperature remains in the hot-working temperature range. This results from the fact that the contact area between the workpiece and the tools is

relatively small, not to mention the considerable amount of heat generated by plastic work. The results demonstrate that the temperature increases locally even up to 50 °C.

Figure 7 shows the axles produced in the rolling tests performed in the CNC skew rolling mill. The axles are shown with machining allowance. The chucking allowance for fixing the workpiece in the four-jaw chuck is shown on the left-hand side. The excess material on the other side of the axle is left for removing the end-face grooves created on the edge of the end step. This defect is typical of cross- and skew rolling processes. It is caused by a rapid flow of material in the surface layers [14, 15]. Figure 8 shows the axles after machining allowance removal and shot peening. This figure also shows the cross sections of the steps on the produced parts. It can be observed that the axles have the required shape and their diameter is within the dimensional tolerance of ± 0.4 mm. The exception is the diameter of the step on the right end of the axle (formed towards the end of the process). This diameter is bigger than the nominal diameter by 0.8 mm. This can be explained by the limited force capacity of the skew rolling mill.

The produced car axles are free from any internal defects such as axial cracks that often occur in cross- and skew rolling processes [16, 17]. On their external surfaces (particularly the tapered one) shallow helical grooves can be noticed, which is characteristic of skew rolling in CNC mills. Future research on the skew rolling process must investigate the

Fig. 5 Skew rolling process for a car axle-type AAR Class E produced in 1:5 scale: **a** cylindrical rod is fed into the workspace of the machine; **b** formation of the step on one workpiece end; **c** rolls are moved over the biggest diameter step, and rolling scale is removed; **d** formation of the central step with variable diameter; **e** formation of the step on the other end of the workpiece; **f** produced axle

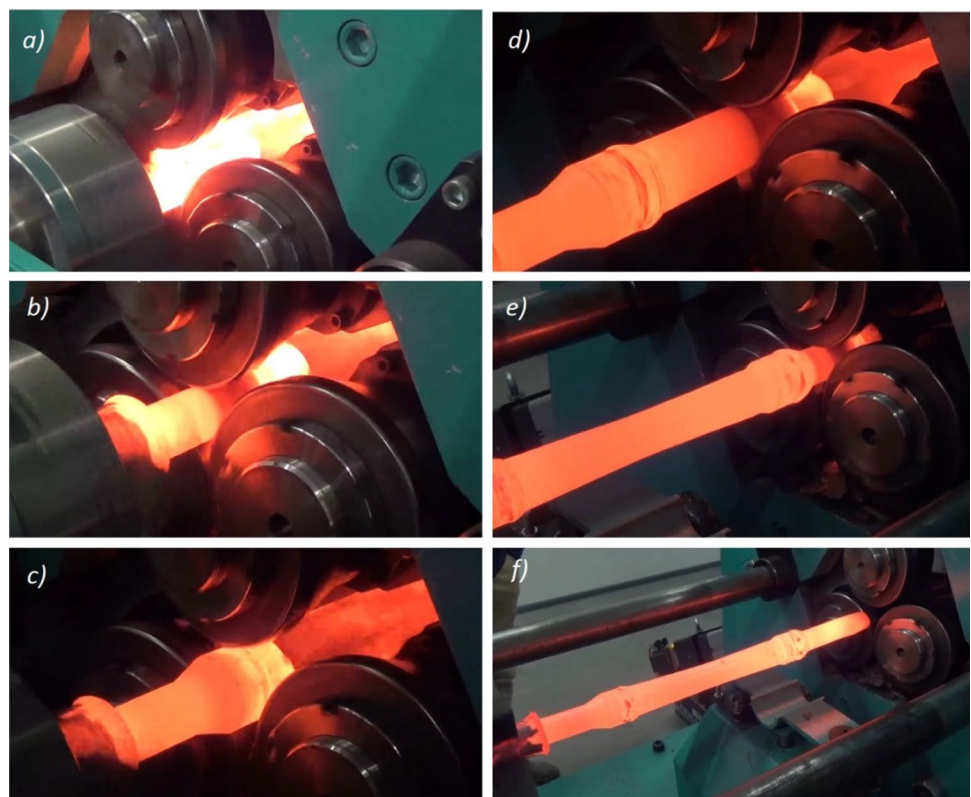


Fig. 6 Infrared thermal imaging of the skew rolling process for an axle-type AAR Class E produced in 1:5 scale in the CNC rolling mill: **a** start of the rolling process; **b** early phase of formation of the central step with variable diameter; **c** final phase of formation of the central step with variable diameter; **d** produced axle

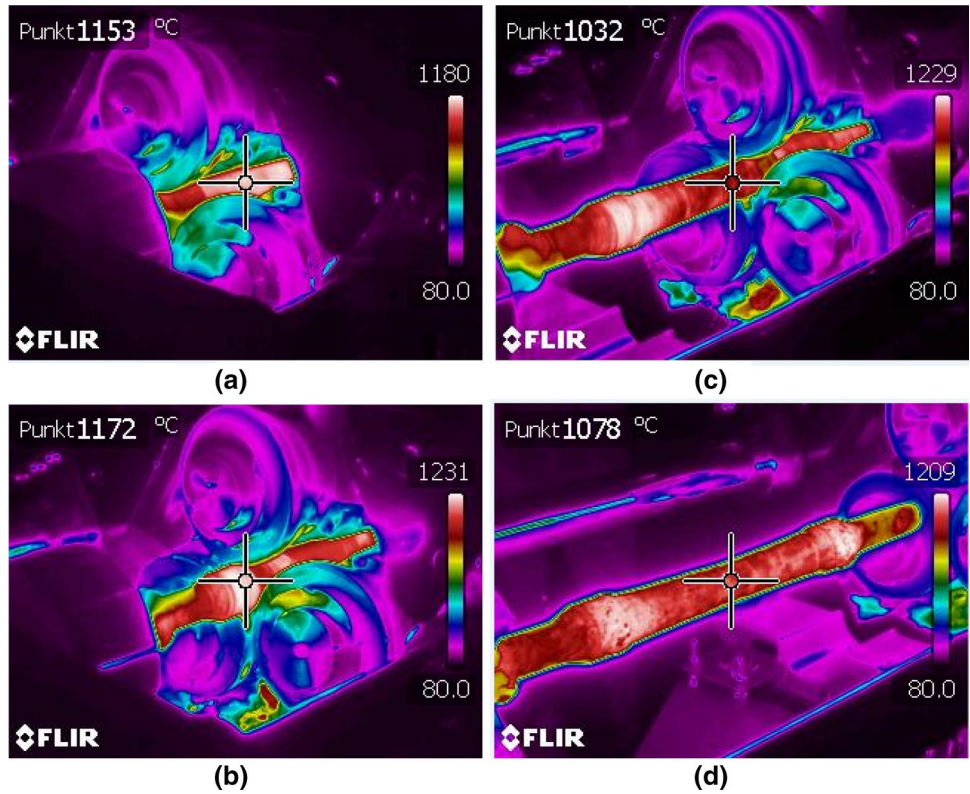


Fig. 7 Car axles manufactured in 1:5 scale in the CNC skew rolling mill: (top) axle-type BA302 (Standard EN 13261); (bottom) axle-type AAR Class E (Standard M101); arrows indicate the regions of increased diameter

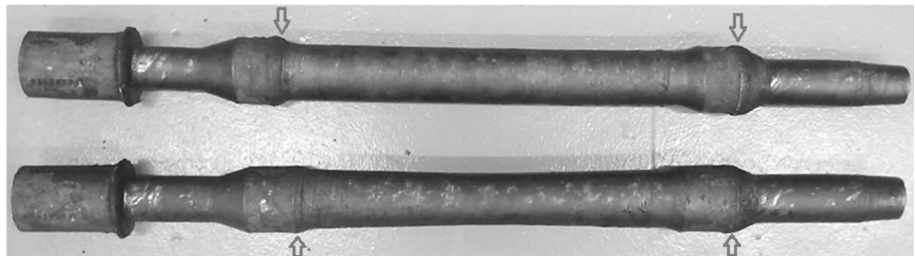
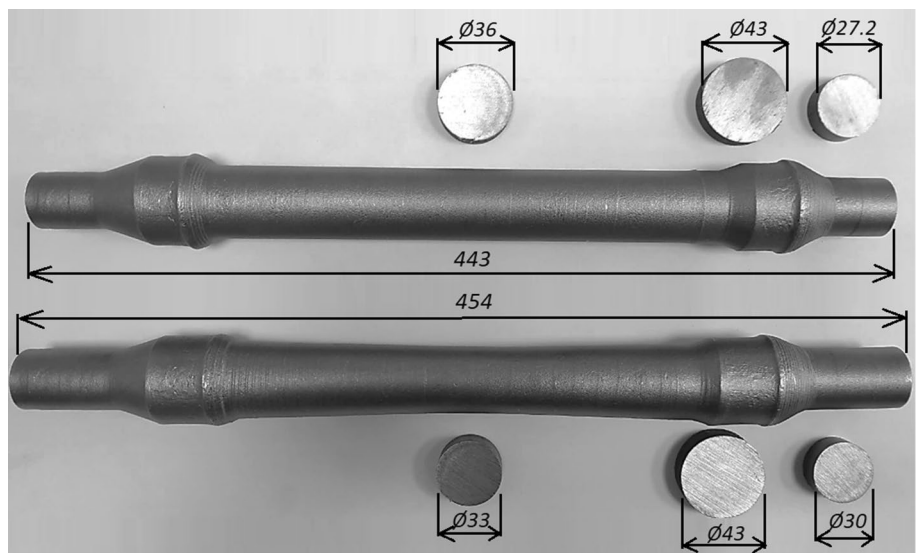


Fig. 8 Rail car axles produced in 1:5 scale after machining allowance removal and shot peening: (top) axle-type BA302 (Standard EN 13261); (down) axle-type AAR Class E (Standard M101)



relationship between the rolling parameters and the occurrence of these surface defects in order to prevent them. Another observed surface defect is a local increase in the diameter of the workpiece (see Fig. 7). This diameter increase is observed in the region of the workpiece where the rolls cut into the material. The observed surface defects are typical of cross-wedge rolling processes [6]. It should however be stressed that these defects do not affect the quality of produced axles in any way, as they are later removed by machining.

Torques and radial loads on the rolls were measured in the rolling process. Figure 9 shows the distributions of torque. The plot clearly demonstrates that the torque strongly depends on the applied diameter reduction. The torque increases with increasing the diameter reduction, and it reaches its maximum values in the final stage of the rolling process. The maximum torque values also depend on the axle type. During the rolling of the European axle the maximum torque is higher than that measured for the axle produced in compliance with the North American standard, which results from the fact that the BA302 axle has a smaller diameter of the end steps. Considering the radial load distributions in the roll shown in Fig. 10, it must be stressed that in terms of quality, they are similar to the torque distributions. It can be observed that in both investigated cases, during the final rolling stage (i.e. when the steps on the workpiece ends are formed), this load reaches the maximum value achievable in the developed rolling mill (i.e. 50 kN). As a result, the diameter of the formed step is 0.8 mm higher than the nominal diameter. The occurrence of the higher radial loads during the formation of the end steps located opposite the chuck (when compared to the steps located near the chuck) can be explained by the fact that the material undergoes cooling, which leads to higher flow stresses. To

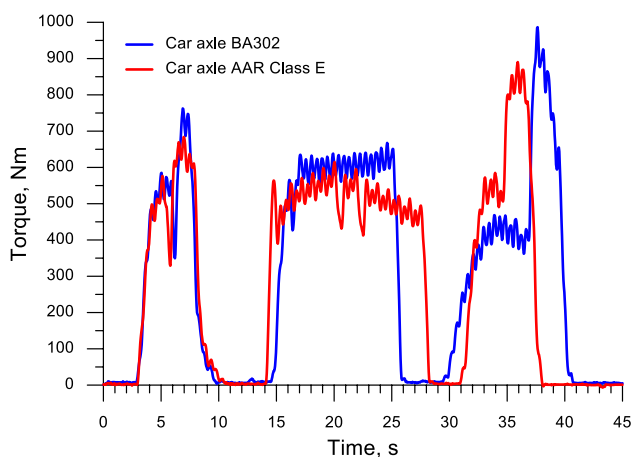


Fig. 9 Torque in the roll in the skew rolling process for rail car axles produced in 1:5 scale

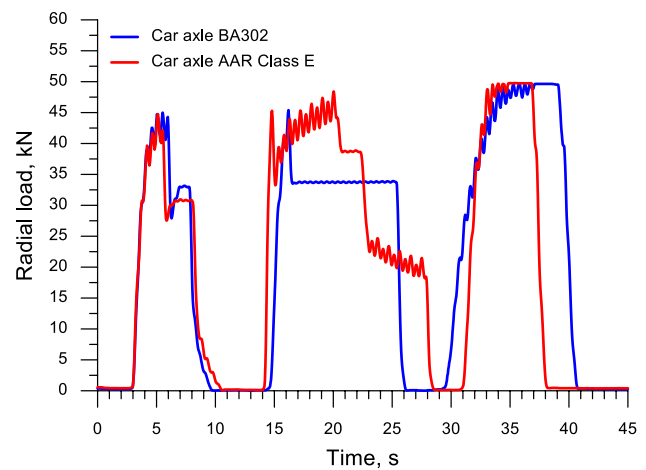


Fig. 10 Radial load in the roll in the skew rolling process for producing rail car axles in 1:5 scale

prevent this, the rolling mill must be redesigned such that the rolling process is performed at higher loads on the rolls.

5 Proposed design of the skew rolling process for rail car axles

A shortcoming of the laboratory skew rolling process for car axles is a considerable amount of chucking allowance (in the rolling process under study it is about 15%). This allowance can be reduced by modifying the existing chuck design. Nevertheless, a better solution is to eliminate the chucking allowance, which can be done with the new method described in the paper. This new method is analysed numerically.

5.1 Numerical model of the skew rolling process for rail car axles

The rolling process for the two analysed types of car axles was modelled numerically using Simufact.Forming v.15. This computer simulation software has been successfully used by many researchers to analyse processes such as cross-wedge rolling [18–20], skew rolling [2, 10, 21–24], and ring rolling [25–27], and the numerical results obtained in these studies were in good agreement with the experimental findings.

The numerical modelling was based on the real dimensions of the tested axles, as specified in Fig. 1. As shown in Fig. 2, the rolls are described by the following parameters: $D = 500$ mm, $b = 25$ mm, and $\alpha = 25^\circ$. During the rolling process, the rolls are positioned askew to the axis of the workpiece at a constant angle $\theta = 5^\circ$ and are rotated in the same direction with a constant speed $n_R = 60$ rpm.

The model of the test material, i.e. 42CrMo4 steel, was described by the following equation (taken from the data library of the Simufact.Forming v.15 software used in the study):

$$\sigma_F = 4628.8e^{-0.00345T} \varepsilon^{(-0.00000509T-0.03638)} e^{(-0.00000461T-0.01944)/\dot{\varepsilon}} \dot{\varepsilon}^{(0.0001893T-0.04627)} \quad (1)$$

where σ_F is the flow stress (MPa), ε is the effective strain (–), $\dot{\varepsilon}$ is the strain rate (s^{-1}), T is the temperature ($^{\circ}C$).

Friction on the contact surface was modelled using the Tresca equation:

$$\tau = mk \quad (2)$$

where τ is the shear stress on the contact surface (MPa), m is the friction factor ($m=0.8$ for the rolls and $m=0.2$ for other tools), k is the yield stress at pure shear ($k = \sigma_F/\sqrt{3}$; MPa).

Thermal effects occurring in the process were also analysed in the numerical simulation. Prior to rolling, the billet was preheated to $1180^{\circ}C$ over its entire volume. The temperature of all tools was maintained constant at $300^{\circ}C$ throughout the rolling process, and the coefficient of heat transfer between the tools and the material was $10 \text{ kW/m}^2\text{K}$.

Cylindrical rods with the dimensions of $\text{Ø}212.6 \times 1695 \text{ mm}$ and $\text{Ø}211 \times 1720 \text{ mm}$ were used for forming the AAR Class E axle and the BA302 axle, respectively. The workpiece was modelled with the use of hexahedral finite elements. The size of a single finite element was set equal to 8 mm. An automatic remeshing tool was used to reconstruct the mesh if the effective strain increased by 0.4. The implicit finite element solver was used to solve the problem.

A schematic design of the proposed method for producing rail car axles is shown in Fig. 11. The novelty of this method lies in the fact that these parts are formed in two operations. The first operation is rolling extrusion [28–30], in which the workpiece is deformed between three rotating rolls. The rolls are positioned such to form the smallest diameter step on the workpiece end. The key parameter in this operation is the pusher velocity v_p , which in both analysed cases was set equal to $v_p = 40 \text{ mm/s}$. The rolls are stopped once the step has been formed on the workpiece end. It should be emphasised that this step must be long enough for fixing the chuck. The pusher is retracted, and the workpiece is fixed in the chuck by the formed step. After that, the rolls are re-started and the chuck is set in translational motion. This marks the beginning of Operation 2 which is performed as a standard CNC skew rolling process [2, 10–13]. According to the proposed solution, the chuck moves with a constant linear velocity $v_c = 50 \text{ mm/s}$, while the velocity of the radially moving rolls is selected such to ensure that products have the required shape.

5.2 Numerical results

Material temperature is a key parameter ensuring that rolling proceeds correctly. Variations in this parameter during

the rolling of a BA302 axle are plotted in Fig. 11. It can be observed that in spite of the relatively long duration of the forming process, the temperature on the workpiece surface remains in the hot-working temperature range. Also, it can be noticed that the temperature increases locally in the workspace of the rolls. This temperature increase is due to the heat generated by deformation work and friction.

An analysis of the temperature variation plots in Fig. 12 provides more information. The plots reveal that the material undergoes local cooling in the region where it is fixed in the chuck. This, however, poses no problems because this part of the workpiece is formed in Operation 1. The temperature in the centre region of the workpiece remains relatively stable, even though it can be noticed that it is slightly higher in the axial region of the workpiece where the heat is not directly carried away to the environment. A different pattern of the temperature variation can be observed with respect to the step located on the other end of the workpiece. This step is formed towards the end of the process. The heat generated at the surface of the material is not yet dissipated over the entire volume of the workpiece, and hence the temperature in the surface layers is higher.

The skew-rolled axles include a small material allowance for end-face grooves on the end steps. This allowance must be removed by machining. An interesting observation is that the depth of the grooves created in Operation 2 (towards the end of the process) is about 35% higher than that of the grooves created in Operation 1 (at the beginning of the process). This probably results from the differences in the friction forces during the rolling extrusion operation and the skew rolling operation.

Figure 13 shows the effective strain distributions in the tested axles. An analysis of the effective strain distributions reveals that the material is deformed on the surface. This is proved by the fact that the effective strains are higher in the surface layers than in the axial region of the products. Also, the bigger the cross-sectional reduction is applied, the higher these strains become, as shown by the plot illustrating the effective strain distribution in the central step of the AAR Class E axle. In addition, the results indicate some differences between the effective strain distributions in the steps on the axle ends. The material in the step formed by rolling extrusion is more worked, which proves that the workpiece elongation process is made difficult due to predominantly radial flow of the material. In contrast, during the forming of

Fig. 11 Skew rolling process for producing an axle-type BA302 in the CNC skew rolling mill modelled in Simufact.Forming, and the temperature distribution in the workpiece

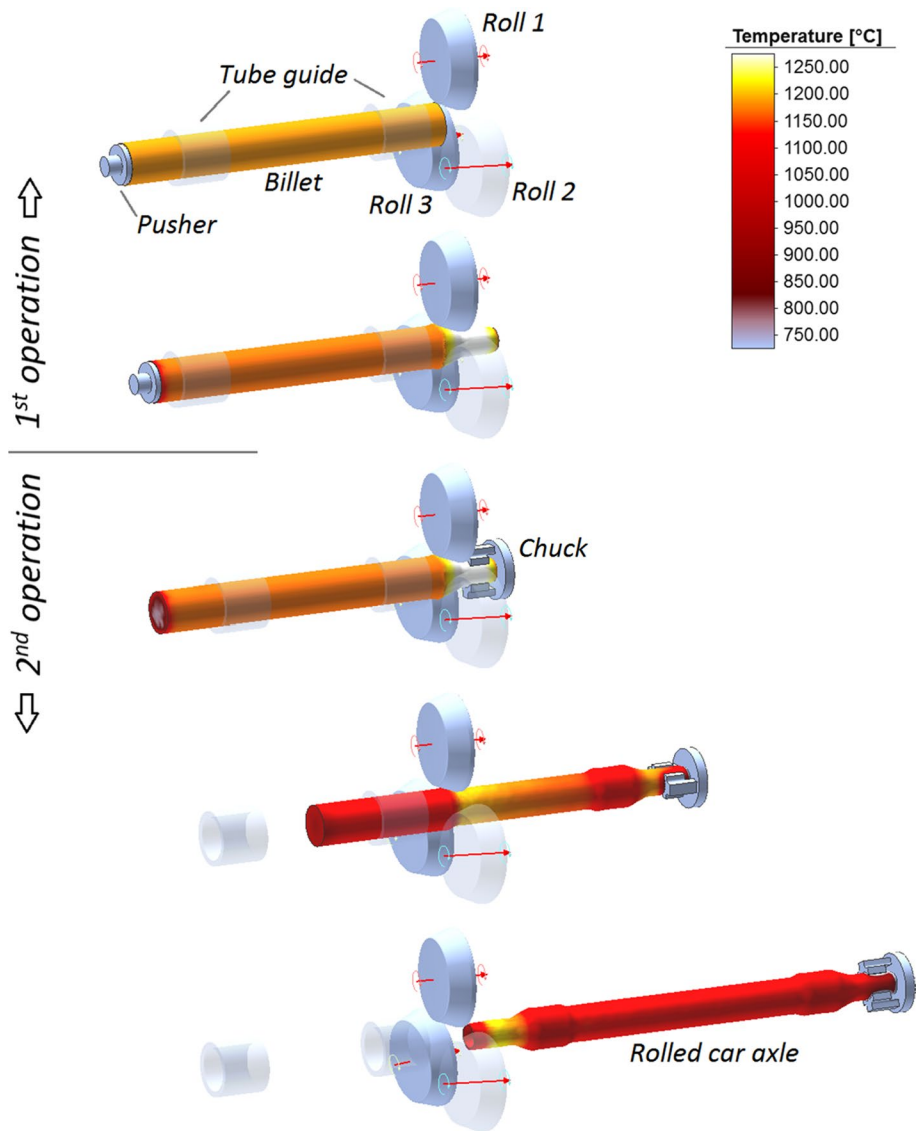
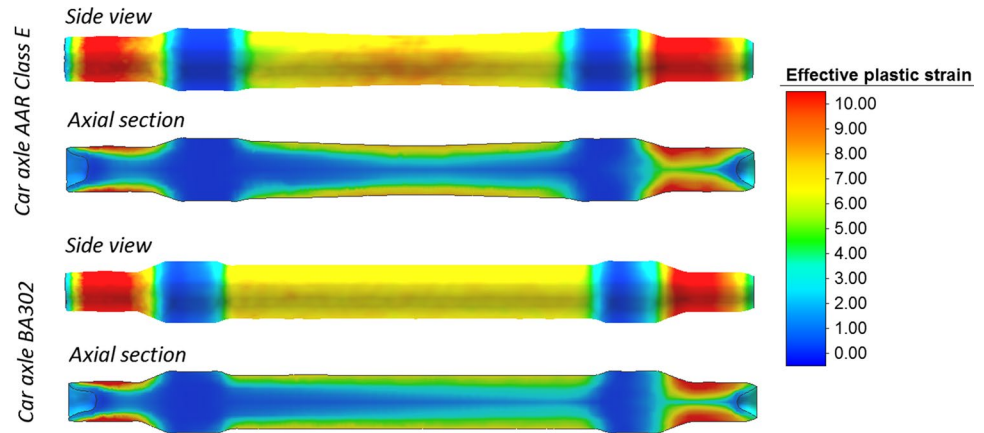


Fig. 12 Temperature distribution in rail car axles produced by skew rolling in the CNC rolling mill



Fig. 13 Effective plastic strain distribution in the rail car axles produced by skew rolling in the CNC rolling mill



the step on the other end of the axle, the material primarily flows on the surface, which results, among other things, in the formation of a deeper groove. It can be stated that the proposed method for producing rail car axles is characterised by low material consumption, and the machining allowance is lower than 5%.

A frequent failure mode in skew rolling is internal cracking primarily in the axial region of the workpiece [31–33]. The occurrence of cracking can be predicted based on damage functions determined by many different criteria. In this study, we used the normalised Cockcroft-Latham ductile damage criterion implemented in the Simufact.Forming program. This criterion reads as follows:

$$\int_0^\epsilon \frac{\sigma_1}{\sigma_i} d\epsilon = C, \tag{3}$$

where σ_i is the equivalent stress, MPa; σ_1 is the maximum principal stress, MPa; C is critical damage value, –.

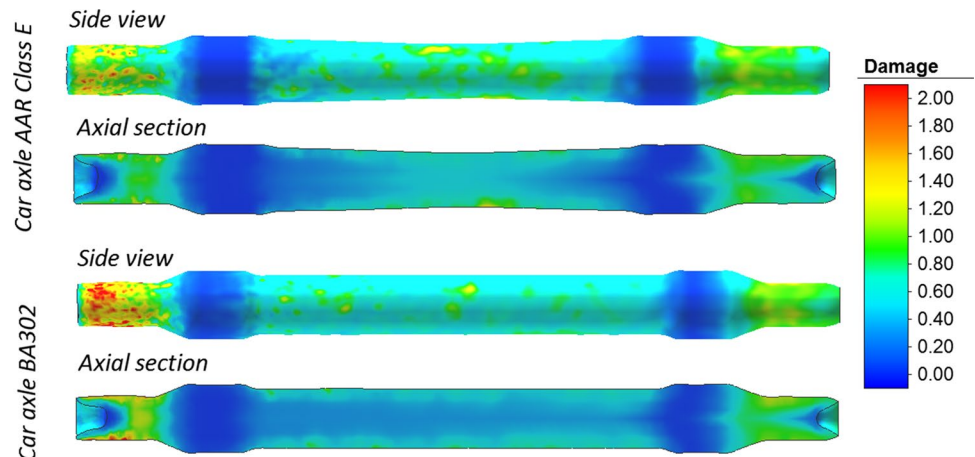
The critical value of damage should be determined by means of a calibration test in which the stress state is as

similar as possible to the stress state occurring in the process being analysed. In our case, the critical damage value can be determined by a channel-die rotational compression test [34]. The critical damage C of C45 steel determined with this test is as high as 3.85 [35].

Figure 14 shows the damage function distributions that were determined in compliance with the normalised Cockcroft-Latham ductile damage criterion. The maximum damage function is observed on the surface of the end step that is formed towards the end of the rolling process. This maximum damage value is approx. 2, which is almost twice lower than the critical value C obtained for C45 steel. This suggests that material cracking should not occur in the forming of axles by the proposed method. To confirm this observation, it is necessary to determine the critical value of damage for 42CrMo4 steel.

The use of numerical modelling made it possible to predict the behaviour of force parameters in the analysed cases. An analysis of the torque distributions shown in Fig. 15 demonstrates that the maximum torque occurs in Operation 1 when the steps on the workpiece ends are formed. This torque increase can be explained by the fact that in Operation

Fig. 14 Damage function distribution (calculated according to the normalised Cockcroft–Latham criterion) in the rail car axles produced by skew rolling in the CNC rolling mill



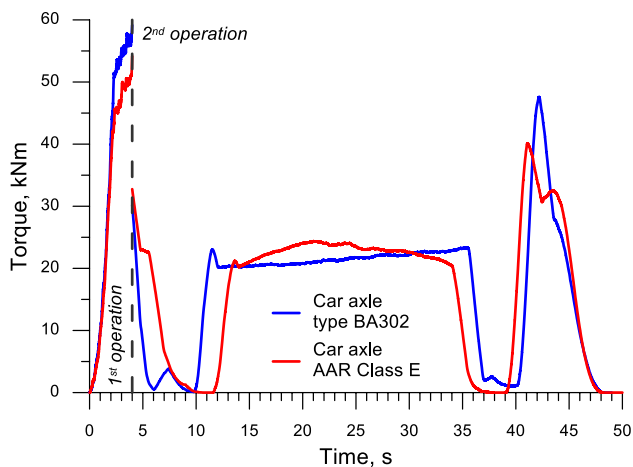


Fig. 15 Torque in the roll in the skew rolling process for rail car axles

1, the velocity of the workpiece upon entering the forming zone ($v_p = 40$ mm/s) is higher than that during the forming of the step on its other end—the workpiece comes out of the rolls with a velocity $v_c = 50$ mm/s. The maximum torque is 60 kNm, which means that the motor power should be 188 kW at least. Hence, it can be assumed that the CNC rolling mill for producing car axles should have a motor power of 200 kW.

Figure 16 shows the radial load distributions in the rolls during the forming process. The highest radial loads are observed during the formation of the end steps of the workpiece, when the maximum cross-sectional reduction takes place. Nevertheless, these loads do not exceed 0.9 MN, which means that the industrial rolling mill for producing car axles can be a relatively lightweight structure.

Figure 17 shows the axial load distributions in the pusher (Operation 1) and in the chuck (Operation 2). The highest

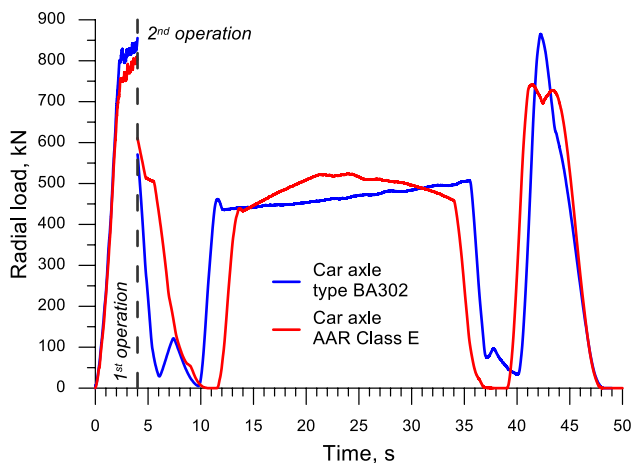


Fig. 16 Radial load in the roll in the skew rolling process for rail car axles

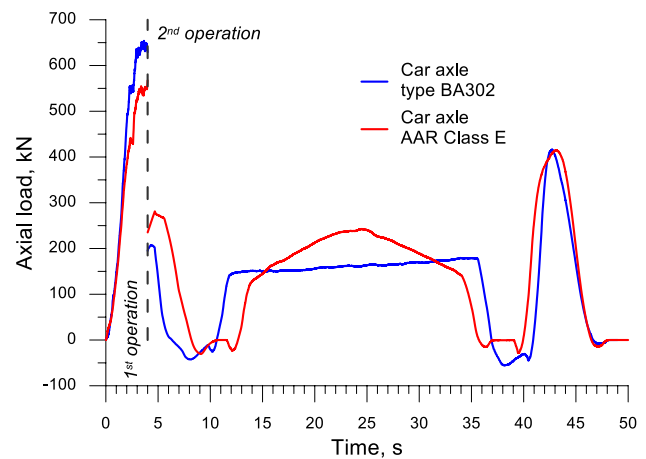


Fig. 17 Axial load in the pusher (Operation 1) and chuck (Operation 2) in the skew rolling process for rail car axles

axial loads can be observed for the pusher and are equal to 550 kN and 650 kN for the BA302 and the AAR Class E axle, respectively. These loads can be decreased (by reducing the velocity v_p , which will also lead to a torque decrease) to the maximum load value obtained for the chuck, which is 400 kN in both analysed cases. An interesting observation is that the chuck load value is negative, as in the case of very small cross-sectional reductions. In effect, the process is spontaneous because the axial force generated due to the skew arrangement of the rolls is high enough to move the workpiece. This means that the workpiece motion is controlled by the chuck and thus the workpiece moves with the required velocity of 50 mm/s.

6 Conclusions

The results of this study lead to the following conclusions:

- Rail car axles can be formed by skew rolling in the CNC rolling mill;
- The diameters of the axles produced in 1:5 scale have an accuracy of ± 0.4 mm;
- Although skew-rolled axles are free from internal cracks, shallow helical grooves are formed on their outer surfaces (the tapered one in particular); these surface defects can easily be removed by machining;
- Despite the relatively long duration of the forming process, the temperature of the material remains in the hot-working temperature range;
- The formation of axles by skew rolling in the CNC rolling mill requires chucking allowance, which, however, leads to a high material loss of up to 15%;
- The material consumption in the forming of rail car axles can be reduced by eliminating the chucking allowance.

This can be done if the forming process is performed in two operations: the rolling extrusion of a step on the workpiece end and the actual skew rolling of an axle;

- The existing CNC skew rolling mill should be redesigned to make it possible to perform the forming process at higher loads (max. 100 kN), in both the rolling extrusion and the skew rolling operation.

Funding The research was financed in the framework of the project Lublin University of Technology-Regional Excellence Initiative, funded by the Polish Ministry of Science and Higher Education (Contract No. 030/RID/2018/19).

Compliance with ethical standards

Conflict of interest The authors declare that they have no conflict of interest.

Open Access This article is licensed under a Creative Commons Attribution 4.0 International License, which permits use, sharing, adaptation, distribution and reproduction in any medium or format, as long as you give appropriate credit to the original author(s) and the source, provide a link to the Creative Commons licence, and indicate if changes were made. The images or other third party material in this article are included in the article's Creative Commons licence, unless indicated otherwise in a credit line to the material. If material is not included in the article's Creative Commons licence and your intended use is not permitted by statutory regulation or exceeds the permitted use, you will need to obtain permission directly from the copyright holder. To view a copy of this licence, visit <http://creativecommons.org/licenses/by/4.0/>.

References

- Shu X, Wei X, Li C, Hu Z. The influence rules of stress about technical parameters on synchronous rolling railway axis with multi-wedge cross-wedge rolling. *Appl Mech Mater*. 2010;37–38:1482–8. <https://doi.org/10.4028/www.scientific.net/AMM.37-38.1482>.
- Xu C, Shu X. Influence of process parameters on the forming mechanics parameters of the three-roll skew rolling forming of the railway hollow shaft with 1:5. *Metalurgija*. 2018;57(3):153–6.
- Kozevnikova GW, Pipicuk GP, Rudovic AO, Schukin VJA. Progressive method of production of raw railway axles. *Tech Zelezných Dorog*. 2017;40(4):31–7 (in Russian).
- Gronostajski Z, Pater Z, Madej L, Gontarz A, Lisiecki L, Łukaszek-Sołek A, et al. Recent development trends in metal forming. *Arch Civ Mech Eng*. 2019;19(3):898–941. <https://doi.org/10.1016/j.acme.2019.04.005>.
- Ji H, Liu J, Wang B, Fu A, Xiao W, Hu Z. A new method for manufacturing hollow valves via cross wedge rolling and forging: numerical analysis and experiment validation. *J Mater Process Tech*. 2017;240:1–11. <https://doi.org/10.1016/j.jmatprotec.2016.09.004>.
- Pater Z. Cross wedge rolling. In: Button ST, editor. *Comprehensive materials processing*, vol. 3. New Work: Elsevier Ltd.; 2014. p. 211–279.
- Peng W, Zheng S, Chiu Y, Shu X, Zhan L. Multi-wedge cross wedge rolling process of 42CrMo4 Large and Long Hollow Shaft. *Rare Metal Mat Eng*. 2016;45(4):836–42. [https://doi.org/10.1016/S1875-5372\(16\)30084-4](https://doi.org/10.1016/S1875-5372(16)30084-4).
- Zheng S, Shu X, Han S, Yu P. Mechanism and force-energy parameters of a hollow shaft's multi-wedge synchrostep cross-wedge rolling. *J Mech Sci Technol*. 2019;33(5):1–10. <https://doi.org/10.1007/s12206-019-0411-1>.
- Pater Z, Tomczak J. A new cross wedge rolling process for producing rail axles. *MATEC Web Conf*. 2018;190:11006. <https://doi.org/10.1051/mateconf/201819011006>.
- Pater Z, Tomczak J, Bulzak T. Numerical analysis of the skew rolling process for rail axles. *Arch Metall Mater*. 2015;60(1):415–8. <https://doi.org/10.1515/amm-2015-0068>.
- Pater Z. FEM analysis of loads and torque in a skew rolling process for producing axisymmetric parts. *Arch Metall Mater*. 2017;62(1):85–90. <https://doi.org/10.1515/amm-2017-0011>.
- Pater Z, Tomczak J, Bulzak T. Numerical analysis of the skew rolling process for main shaft. *Metalurgija*. 2015;54(4):627–30.
- Pater Z, Tomczak J, Bulzak T. Numerical analysis of a skew rolling process for producing a stepped hollow shaft made of titanium alloy Ti6Al4V. *Arch Metall Mater*. 2016;61(2):677–82. <https://doi.org/10.1515/amm-2016-0115>.
- Wei J, Shu X, Tian D, et al. Study in shaft end forming quality of closed-open cross wedge rolling shaft using a wedge block. *Int J Adv Manuf Technol*. 2017;93(1–4):1095–105. <https://doi.org/10.1007/s00170-017-0507-7>.
- Pater Z, Tomczak J, Bulzak T. Cavity formation in cross-wedge rolling processes. *J Iron Steel Res Int*. 2019;26(1):1–10. <https://doi.org/10.1007/s42243-018-0075-6>.
- Yang C, Dong H, Hua Z. Micro-mechanism of central damage formation during cross wedge rolling. *J Mater Process Tech*. 2018;252:322–32. <https://doi.org/10.1016/j.jmatprotec.2017.09.041>.
- Pater Z, Tomczak J, Bulzak T. Establishment of a new hybrid fracture criterion for cross wedge rolling. *Int J Mech Sci*. 2020;167:105274. <https://doi.org/10.1016/j.ijmecsci.2019.105274>.
- Huang H, Chen X, Fan B, Jin Y, Shu X. Initial billet temperature influence and location investigation on tool wear in cross wedge rolling. *Int J Adv Manuf Tech*. 2015;79:1545–56. <https://doi.org/10.1007/s00170-015-6882-z>.
- Tofil A, Tomczak J, Bulzak T. Numerical and experimental study on producing aluminum alloy 6061 shafts by cross wedge rolling using a universal rolling mill. *Arch Metall Mater*. 2015;60(2):801–7. <https://doi.org/10.1515/amm-2015-0210>.
- Pater Z, Tomczak J, Bulzak T. Cross-wedge rolling of driving shaft from titanium alloy Ti6Al4V. *Key Eng Mat*. 2016;687:125–32. <https://doi.org/10.4028/www.scientific.net/KEM.687.125>.
- Lis K, Wójcik Ł, Pater Z. Numerical analysis of a skew rolling process for producing a crankshaft preform. *Open Eng*. 2016;6:581–4. <https://doi.org/10.1515/eng-2016-0087>.
- Pater Z, Tomczak J, Bartnicki J, Lovell MR, Menezes PL. Experimental and numerical analysis of helical-wedge rolling process for producing steel balls. *Int J Mach Tool Manu*. 2013;67:1–7. <https://doi.org/10.1016/j.ijmactools.2012.12.006>.
- Tomczak J, Pater Z, Bulzak T. Designing of screw impressions in helical rolling of balls. *Arch Civ Mech Eng*. 2014;14:104–13. <https://doi.org/10.1016/j.acme.2013.07.004>.
- Cao Q, Hua L, Qian D. Finite element analysis of deformation characteristics in cold helical rolling of bearing steel-balls. *J Cent South Univ*. 2015;22:1175–83. <https://doi.org/10.1007/s11771-015-2631-6>.
- Berti GA, Quagliato L, Monti M. Set-up of radial-axial ring-rolling process: process worksheet and ring geometry expansion prediction. *Int J Mech Sci*. 2015;99:58–71. <https://doi.org/10.1016/j.ijmecsci.2015.05.004>.

26. Quagliato L, Berti GA. Mathematical definition of the 3D strain field of the ring in the radial-axial ring rolling process. *Int J Mech Sci.* 2016;115–116:746–59. <https://doi.org/10.1016/j.jmesci.2016.07.009>.
27. Quagliato L, Berti GA, Kim D, et al. Contact geometry estimation and precise radial force prediction for the radial-axial ring rolling process. *Int J Mater Form.* 2018;11:789–805. <https://doi.org/10.1007/s12289-017-1388-x>.
28. Bartnicki J, Pater Z, Gontarz A. Theoretical analysis of rolling-extrusion process of axi-symmetrical parts. *Arch Civ Mech Eng.* 2008;8(2):5–11. [https://doi.org/10.1016/S1644-9665\(12\)60188-5](https://doi.org/10.1016/S1644-9665(12)60188-5).
29. Neugebauer R, Kolbe M, Glab R, Hoffmann M. Optimisation of processing routes for cross rolling and spin extrusion. *J Mater Process Tech.* 2002;125–126:856–62. [https://doi.org/10.1016/S0924-0136\(02\)00392-8](https://doi.org/10.1016/S0924-0136(02)00392-8).
30. Neugebauer R, Kolbe M, Glab R. New warm forming processes to produce hollow shafts. *J Mater Process Tech.* 2001;119:277–82. [https://doi.org/10.1016/S0924-0136\(01\)00939-6](https://doi.org/10.1016/S0924-0136(01)00939-6).
31. Yang C, Zhang K, Hu Z. Development of central minute cavity in the workpiece of cross wedge rolling. *Appl Mech Mater.* 2012;215–216:766–70. <https://doi.org/10.4028/www.scientific.net/AMM.215-216.766>.
32. Yang C, Dong H, Hu Z. Micro-mechanism of central damage formation during cross wedge rolling. *J Mater Process Techn.* 2018;252:322–32. <https://doi.org/10.1016/j.jmatprotec.2017.09.041>.
33. Pater Z, Tomczak J, Bulzak T, Wójcik Ł, Walczuk P. Assessment of ductile fracture criteria with respect to their application in the modeling of cross wedge rolling. *J Mater Process Techn.* 2020;278:116501. <https://doi.org/10.1016/j.jmatprotec.2019.116501>.
34. Pater Z, Walczuk P, Lis K, Wójcik Ł. Preliminary analysis of a rotary compression test. *Adv Sci Technol Res J.* 2018;12(2):77–82. <https://doi.org/10.12913/22998624/86812>.
35. Pater Z, Tomczak J, Bulzak T, Bartnicki J, Tofil A. Prediction of crack formation for cross wedge rolling of harrow tooth preform. *Materials.* 2019;12:2287. <https://doi.org/10.3390/ma12142287>.

Publisher's Note Springer Nature remains neutral with regard to jurisdictional claims in published maps and institutional affiliations.